Desalination and Water Treatment
www.deswater.com

doi:10.5004/dwt.2018.23170

132 (2018) 287–296
November

Comparative assessment on the removal of ranitidine and prednisolone present in solution using graphene oxide (GO) nanoplatelets

Suparna Bhattacharyya[a], Priya Banerjee[b], Sandipan Bhattacharya[a], Rishi Karan Singh Rathour[c], Subrata Kumar Majumder[d], Papita Das[a,*], Siddhartha Datta[a]

[a]*Department of Chemical Engineering, Jadavpur University, Kolkata - 700032,India, email: suparna.ch2015@gmail.com (S. Bhattacharyya), sandipan.bhattacharya0@gmail.com (S. Bhattacharyya), papitasaha@gmail.com (P. Das), sdatta.che@gmail.com (S. Datta)*
[b]*Department of Environmental Studies, Rabindra Bharati University, Directorate of Distance Education, Kolkata, email: prya_bnrje@yahoo.com (P. Banerjee)*
[c]*School of Environmental Science and Engineering, Indian Institute of Technology – Kharagpur, email: rrathour@iitkgp.ac.in (R.K.S. Rathour)*
[d]*Department of Chemical Engineering, Indian Institute of Technology Guwahati, Guwahati-781039, Assam, India, email: skmaju@iitg.ac.in (S.K. Majumder)*

Received 16 April 2018; Accepted 17 September 2018

ABSTRACT

In recent times, pharmaceutical wastes are becoming major water pollutants responsible for water borne diseases and drastic alterations of aquatic ecological cycle. In this present study, graphene oxide (GO) nanoplatelets are synthesize during graphite as the parent substrate. The GO so prepared has been further investigated for removal of pharmaceuticals like ranitidine and prednisolone from their respective aqueous solutions. Batch studies were performed for determining the effect of significant process parameters like adsorbent dose, temperature, solution pH and agitation speed on the process of adsorption. The adsorbent and the process of sorption have been thoroughly characterized and explained on the basis of scanning electron microscopy (SEM), Fourier transform infrared spectroscopy (FTIR), X-ray diffractometry (XRD) and Raman spectroscopy. Results obtained in this study have also been used for analysis of process isotherms(like Langmuir, Freundlich, Temkin and D-R)and kinetics. Thermokinetics of the spontaneity of the reaction was also determined. Process optimization was performed with artificial neural network modeling. Regeneration potential of the adsorbent was also determined in order to understand the reusability of the adsorbent.

Keywords: Pharmaceuticals; Graphene oxide; Artificial neural network; Process isotherm and kinetics; Thermodynamics; Adsorbent characterization

1. Introduction

In recent times, pharmaceutical wastes are being considered as harmful bioactive chemicals capable of drastic pollution of our environment. Discharge of these toxic substances is contaminating water bodies and the neighboring ecosystems alike, but is yet to be addressed in a proper manner. Several processes are presently being investigated for management of these pollutants [1]. These pollutants are continuously introduced in the environment through several pharmaceutical industries, hospital and domestic wastes. These contaminants exert harmful effects on both aqueous ecosystems and human health [2,3]. The therapeutic drugs and prescribed compounds used are considered as primary causes of health issues arising from consumption of water contaminated with the same. Moreover, chemicals, disinfectants, fragrances and veterinary drugs also have detrimental effects on the water bodies they are discharged into [4,5]. Thus development of an efficient process for removal of these toxic substances from water has emerged as a major concerning issue [6–8].

Some of the existing technologies for treatment of toxic pollutant bearing effluents include coagulation [9], floatation [10], filtration [11], ion exchange [12,13], advanced oxi-

*Corresponding author.

dation processes [14], solvent extraction [15], electrolysis [16], adsorption [17,18], ultra filtration [19], nanofiltration [19] and Fenton oxidation [20]. In comparison to all other existing technologies, adsorption has been reportedly considered to be the most effective removal technique due to its simple application and low cost incurred. However, different adsorbents reported so far have not been appreciatively efficient or cost effective for wide scale application.

Recent studies have revealed that nanomaterials have been capable of efficient removal of similar pharmaceuticals primarily due to their unique structure and properties. The high surface area of such nanomaterials (like carbon nanotubes) facilitates efficient adsorption of organic pollutants there by providing a new prospect for the management of such pharmaceutical wastes. Review of recent literature revealed that graphene, graphene oxide and several other graphene derivatives have demonstrated exciting features of adsorption that has been found to be even better in comparison to carbon nanotubes. Being an oxidative derivative of graphene, graphene oxide (GO) is having oxygen containing functional groups like hydroxyl and epoxy group on the basal planes and carbonyl and carboxylic groups at the edges.

Recent studies have reported functionalized graphene and its different oxidized and reduced form to adsorb different kinds of pharmaceutical and complex organic chains present within the hospital run-off and pharmaceutical debris. Adsorption of several aromatic pharmaceutical wastes has been reported using sulfonated graphene [21]. Removal of 4-n-Nonylphenol and Bisphenol-A has been carried out by magnetic reduced GO [22]. Adsorption of benzene, aniline and naphthylamine has been reportedly performed using reduced GO [23]. Magnetite–GO and magnetite-reduced GO composites have also been reported for removal of As(III) and As(V) [24].

The large theoretical specific area (2620 $m^2 g^{-1}$) and oxygenated functional groups present on the surface of graphene oxide has been reportedly considered as primary features facilitating potential adsorption of organic pollutants like pharmaceutical wastes [21–23]. Therefore, graphene oxide has been investigated for clean up of environmental pollution [25]. The large specific surface area of GO has been attributed to its one-atom thickness and two-dimensional planar. GO has been reportedly performing drug removal by surface adsorption, hydrogen bonding and other types of interactions [26,27].

The present study primarily investigated the adsorption of pharmaceutical wastes like ranitidine and prednisolone from their aqueous solution by using graphene oxide nanoplatelets as an adsorbent. Several studies have previously investigated the removal of ranitidine and prednisolone using other adsorbents like activated carbon prepared from mung bean husk [5] and rice bran derivative [28,29] as well as other [6,12]. Very few recent studies have investigated the removal of complex and harmful pharmaceutical wastes like ranitidine and prednisolone with high adsorption efficiency using nanomaterials like GO. Therein lies the uniqueness and importance of the present study.

In the present study, batch studies were carried out to determine the effect of various experimental parameters like adsorbent dose,temperature,solution pH and agitation speed. The selected experimental parameters were further optimized by artificial neural network analysis (ANN). ANN is a computing process which can be used for solving the complex problem [30]. The basic structure of ANN comprises of an input layer (independent variables), number of hidden layers and an output layer (dependent variables). These layers comprises of number of interconnected processing unit and neurons remain connected by sending signals to each other. The mechanism of adsorption was elucidated in terms of adsorption isotherm, kinetics and thermodynamics as well as a detailed physic-chemical characterization of the adsorbent used.

2. Material and methods

2.1. Reagents used

Ranitidine ($C_{13}H_{22}N_4O_3S$), commercially available as Zantac and Prednisolone ($C_{21}H_{28}O_5$) were commercially obtained from Sigma Aldrich and used as received. Other chemicals like graphite powder, sodium hydroxide (NaOH), hydrochloric acid (HCl; 37%), potassium permanganate ($KMnO_4$), sulfuric acid (H_2SO_4; 98%) and hydrogen peroxide (H_2O_2; 30%) were purchased from Merck, India and used for synthesis of GO. All chemicals used in this study were of analytical grade.

2.2. Preparation of adsorbent

GO nanoplatelets used in the present study were synthesized using modified Hummer's Method [31]. In this process graphite powder was added to H_2SO_4(98%) and the mixture was continuously stirred with the help of a glass rod in an ice-bucket with gradual addition of required quantity of $KMnO_4$. About 100 ml of distilled water was then slowly added to this mixture and subjected to stirring for 180 min at 40°C. After 180 min, another 100 ml of distilled water was added slowly to the reaction mixture by placing the same on an ice tray. Post the addition of distilled water, H_2O_2 and was added to the reaction mixture which in turn yielded brownish yellow slurry. For obtaining uniform particle size, the slurry was exposed to with ultrasound irradiation for 15 min [31]. Afterwards,the mixture treated by ultrasound was centrifuged and the precipitate was repeatedly washed with de-ionized water for surface neutralization. Finally the washed product was dried in a hot air oven (SICCO,India) at 60°C for 10 h, ground, sieved and stored for use as adsorbent.

2.3. Preparation of adsorbate

Adsorbate (Ranitidine and Prednisolone) stock solution was prepared by dissolving required amount of the drug (100 mg/L) in distilled water. Then working solutions of desired concentrations were prepared by diluting the stock solution with distilled water as required. Finally, a standard curve was generated using adsorbate solutions of known concentrations.

2.4. Batch study

The batch adsorption experiment was carried out in 250 mL conical flasks with 100 mL adsorbate solution of

10 mg/L concentration. These working solutions were used for determining the effect of variations of different parameters like adsorbent (GO) dosage (0.5,0.75, 1.0,2.0 g/L), temperature (298, 303, 308, 313 K), pH (2, 4, 6, 8) over contact time (15, 30, 45, 60, 120 min) respectively. The flasks containing the working solutions were maintained in a temperature controlled incubator shaker (S.C. Dey & Co, India). After specified time intervals, samples were collected from the flasks and centrifuged using Plasto Crafts Centrifuge. The supernatants were tested for residual drug concentration using a UV visible spectrophotometer (Lambda 25 Perkin Elmer). Before each experiment, the pH of the working solutions were adjusted by the addition of 1.0 M NaOH or 0.1 N HCl as required [31].

2.5. Measurement of residual adsorbate concentrations in solution

A calibration curve of the used adsorbate (ranitidine and prednisolone) was plotted, taking the concentration range of 2–10 mg/L. A double beam UV-Visible spectrophotometer (Perkin Elmer Lambda 25, USA) was used to determine the adsorbate concentration of the standards, untreated and treated effluents. All samples were centrifuged before the analysis in order to minimize the any interference caused by fine GO particles. The treated adsorbate solutions were centrifuged and the supernatants obtained were used for determining residual adsorbate concentration [31].

2.6. Characterization of adsorbent

The morphological properties of GO were determined with a scanning electron microscope (SEM, ZEISSEV-OMA10, Germany). Prior to performing the SEM analysis, the samples were gold coated with a sputter coater for making the same conductive [26].

Fourier transform infrared (FTIR) spectroscopy was performed to identify the chemical bonds in a molecule by producing an infrared absorption spectrum. FTIR analysis of GO was done by casting the same into pellets using potassium bromide (KBr) and GO in a ratio of 100:1 (w/w). The pellets were then analyzed using a FTIR spectrometer (Perkin Elmer) with a resolution of 4 cm^{-1} [31].

The adsorbent was also subjected to XRD analysis for investigating the interlayer spacing of the prepared GO. Results of the XRD analysis were recorded using a diffractometer with Cu $K\alpha$ radiation operating at 40 kV potential difference and 40 mA current over the range (2θ) of 5–80° [32].

Samples were also analyzed using Raman spectroscopy (Model: T64000, Make: J-Y Horiba) for evaluation of the degree of structural deformations and number of layers in the prepared GO [22,25].

2.7. ANN model

In this study, the inputs selected for the ANN model were parameters like adsorbent dose, temperature, solution pH and agitation speed. The neural network toolbox of MATLAB version 7(R2013b) was engaged for carrying out the ANN calculations [30].

Artificial neural network (ANN) is a tool for mathematical modeling used for solving complex problems that are related with the field of modeling and optimization. High operational performance can be achieved using this mathematical tool [28]. The schema of the model is similar to that of human brain function, its interlinks and connections. It mainly comprises of three functional groups, outside signal receiver, the processing neurons which process the information and the result generating neurons [29]. Mainly there are three layers in the model of multi-layered perception neural network consisting of input, output and one or more hidden layers. Sum of the weighted values provided as the input layer undergo modification by a sigmoid transfer function to produce an output. Data processing is done in the hidden layer. A tan-sigmoid transfer function (tansig) at hidden layer and a linear transfer function (purelin) at output layer was studied in combination with the Levenberg–Marquardt back-propagation (Trainlm) algorithm for network training [28,33].

3. Theoretical calculation

3.1. Equilibrium concentration study and percent removal (%) of adsorbate

The calculation of the percentage removal for each drug was performed with the following equation:

$$Removal(\%) = \frac{C_i - C_e}{C_i} \times 100 \tag{1}$$

The adsorption capacity of GO was calculated using the following mass balance equation:

$$q_e = \frac{(C_i - C_e)V}{m} \tag{2}$$

3.2. Isotherm analysis

The isotherm study was performed to identify the isotherm model guiding the process of adsorption investigated in this study. Tested isotherms included the Langmuir, Freundlich, Temkin and Dubinin-Radushkevich (D-R) isotherm models. This study can also determine the equilibrium relationship between the adsorbate concentration in the liquid phase and that on the adsorbent's surface under a given condition.

3.2.1. Langmuir isotherm

Langmuir isotherm equation is given by

$$\frac{1}{q_e} = \frac{1}{q_{\max}} + \left(\frac{1}{q_{\max} K_L}\right).\frac{1}{C_e} \tag{3}$$

where K_L (L/mg) is obtained when $1/q_e$ was linearly plotted against $1/C_e$. This isotherm denotes monolayer sorption of adsorbate on the available surface of the adsorbent [33].

3.2.2. Freundlich isotherm

The equation of the Freundlich isotherm model is expressed as follows:

$$\ln(q_e) = \ln(K_F) + \frac{1}{n}\ln(C_e) \tag{4}$$

The bonding energy and the amount of adsorbate adsorbed by the adsorbent are mainly highlighted by the Freundlich isotherm model [32,33].

3.2.3. D- R isotherm

The D-R isotherm is expressed by the following equations:

$$\ln(q_e) = \ln(q_m) - \beta\varepsilon^2 \quad (5)$$

$$\varepsilon^2 = RT \ln\left(1 + \frac{1}{C_e}\right) \quad (6)$$

Information regarding the porosity, free energy and the maximum adsorption capacity of the adsorbent are provided by the D-R isotherm model. The slope and intercept of the ln q_e vs. ε^2 plot represent the activity coefficient (β; $mol^2/K/J^2$) and maximum adsorption capacity (q_m; mg/g) respectively. Using the values of β obtained from D-R isotherms recorded at different temperatures (293–308 K), the mean sorption energy (E; KJ/mol) was calculated as follows:

$$E = \frac{1}{\sqrt{2\beta}} \quad (7)$$

3.2.4. Temkin isotherm

The Temkin isotherm is expressed by the following equation:

$$q_e = BlnA_T + BlnC_e \quad (8)$$

The Temkin isotherm model provides an insight into the type of interaction occuring between the adsorbate and adsorbent moities [33].

3.3. Kinetic analysis

The experimental data were interpreted by three kinetic models, i.e. the pseudo first-order equation, the pseudo second order equation and an intra particle diffusion equation [33].

3.3.1. Pseudo first order kinetics

The pseudo first-order rate expression [34] is given as follows:

$$\frac{1}{q_t} = \left(\frac{k_1}{q_1}\right).\left(\frac{1}{t}\right) + \frac{1}{q_1} \quad (9)$$

The pseudo first order rate constant (k_1) was derived from the linear plots of *log* ($q_e - q_t$) vs. *t*.

3.3.2. Second order reaction

The pseudo-second-order kinetic model [35] is expressed as follows:

$$\frac{t}{q_t} = \frac{1}{k_2.q_2^2} + \frac{1}{q_1}t \quad (10)$$

The pseudo second order rate constant (k_2) was derived from the linear plots of t/q_t vs. *t*.

3.3.3. The intra-particle diffusion reaction

The intra-particle diffusion equation [36] is expressed as follows:

$$q_t = k_p \cdot t^{\frac{1}{2}} + C \quad (11)$$

The constant (*C; mg/g*) and intra particle diffusion rate constant (K_{diff}; *mg/g/min*$^{1/2}$) were indicated by the intercept and slope of the regression plot q_t vs. $t^{1/2}$ respectively.

3.4. Thermodynamic analysis

The thermodynamic parameters such as Gibbs free energy (ΔG°), enthalpy (ΔH°), and entropy (ΔS°) were determined using the following equations [33]:-

$$K_C = \frac{C_A}{C_S} \quad (12)$$

$$\Delta G^o = -RTlnK_C \quad (13)$$

$$\ln K = \frac{\Delta S^o}{R} - \frac{\Delta H^o}{RT} \quad 14)$$

The q_e of the pseudo second order model was used to derive the values of C_A and C_S. ΔH°and ΔS° were calculated from the slope and intercept of the Van't Hoff plot of lnK_C vs. *1/T* [33].

4. Results and discussions

4.1. Characterization of the graphene oxide (GO)

SEM, FTIR, XRD and Raman spectroscopic analysis have been performed for characterization of the GO used as an adsorbent in this study. Fig. 1a shows structural and morphological properties of GO recorded with SEM. The SEM images revealed GO to bea disordered solid of in-distinctly aggregated, thin,closely associated and highly overlapping sheets. The exposed surfaces of the crumpled GO sheets reportedly facilitate efficient adsorption [31,32,34]. The wrinkled and layered structures of GO arise due to the interactions between oxygen containing functional groups [37–39]. The functional groups present on the GO surface were investigated by FTIR analysis [figure not shown]. The characteristic peaks obtained at 1366 cm^{-1} and 1636 cm^{-1} indicated stretching of C=C and C-O bond respectively. Moreover, peaks recorded at 2926 cm^{-1} and 3499 cm^{-1} indicated alkyl stretching of C-H bond and C=C bonding respectively in freshly prepared GO [37–39].

XRD analysis of GO is presented in Fig 1b. Three peaks at 10.5, 26.60 and 43.09 denote characteristics peaks of GO and indicate successful synthesis of the same [32,34,38,39].

Raman spectroscopy revealed the difference of graphitic plane that can be determined from the intensity ratio between the D band and G band (I_D/I_G). Raman analysis indicated [Fig. 1c] that the G band is observed at 1572 cm^{-1},

1592 cm^{-1}, and the D band at 1346 cm^{-1}, 1348 cm^{-1}, for graphite and GO, respectively. Analysis of all the spectra indicated that the G band is shifted to a higher wave number after introduction of oxygenated functional groups to graphite and from the conversion of sp^2 types of carbons into sp^3 carbon atoms [23]. The analysis also indicated the broadening of the D band in GO after oxygenation of graphite. The I_D/I_G ratio was found to increase from 0.26 (graphite) to 1.13 (GO) indicating that oxygen containing functional groups had been grafted on the graphitic planes [21–25].

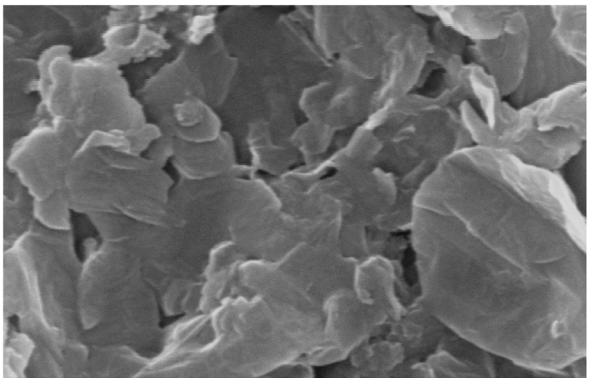

Fig. 1.(a). Graphene oxide structure under SEM analysis.

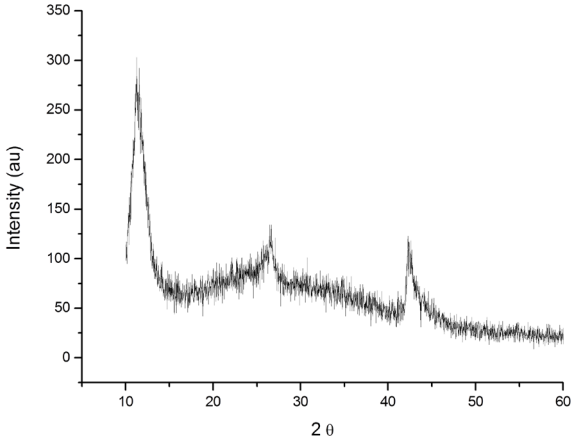

Fig. 1. (b). XRD analysis of Graphene oxide.

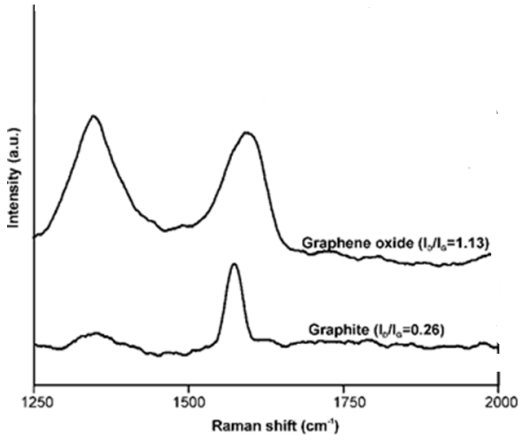

Fig. 1. (c). Raman analysis of Graphene oxide and graphite.

4.2. Batch studies

4.2.1. Effect of adsorbent dose

As evident from Fig. 2, adsorbate removal was found to increase from 55.31% to 94.06% in case of Ranitidine and 29.76% to 87.56% in case of Prednisolone as the adsorbent dosage was increased from 0.50–2.00 g/L. Results obtained indicated that addition of 2 g/L of GO as adsorbent was responsible for maximum removal of both the adsorbate. On addition of 2 g/L of GO, the maximum percentage removal of Ranitidine and Prednisolone were found to be 94.06% and 87.56% respectively.

Similar behavior was also reported in previous studies [28,31,40]. In every cases adsorption efficiency increased with increasing adsorbent dosage. The reason behind it may be that with an increase in adsorbent dosage, the surface area for adsorbing these adsorbate molecules became larger. Thus, the available pores engulfed higher amounts of adsorbate, thereby resulting in a corresponding rise in the adsorption efficiency of the GO used.

4.2.2. Effect of temperature

Temperature is one of the most important controlling parameter for the process of adsorption. For a particular adsorbate, equilibrium capacity is greatly affected by temperature. So the effect of temperature for the removal of both the drugs using GO as an adsorbent, was examined over a range of 298 K–313 K. Within this range, the maximum percentage drug removal was recorded at 313 K for both the drugs, keeping all other parameters constant.

Results shown in Fig. 3 indicate that the percentage drug removal had increased from 74.06 to 94.06% for ranitidine and 36.3–92.68% for prednisolone with a corresponding increase in temperature. This increase of rate of adsorption with temperature also confirmed the endothermic nature of the adsorption process. The highest percentage removal was found to be 94.063% and 92.68% for ranitidine and prednisolone respectively. The increase in % drug removal with a corresponding rise in temperature may have been

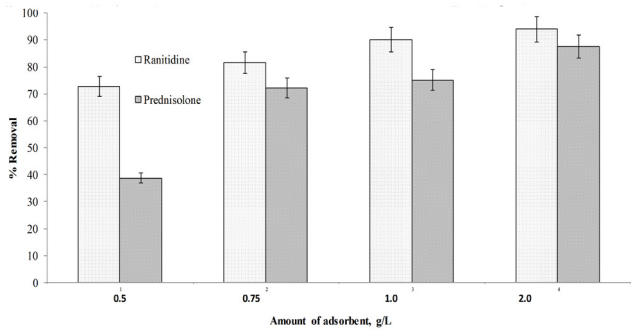

Fig. 2. Effect of various adsorbent dose on the removal of ranitidine and prednisolone.

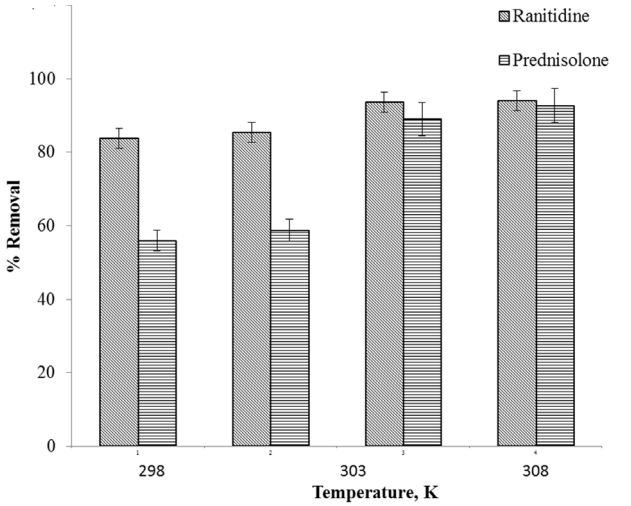

Fig. 3. Effect of temperature on the removal of ranitidine and prednisolone present in solution.

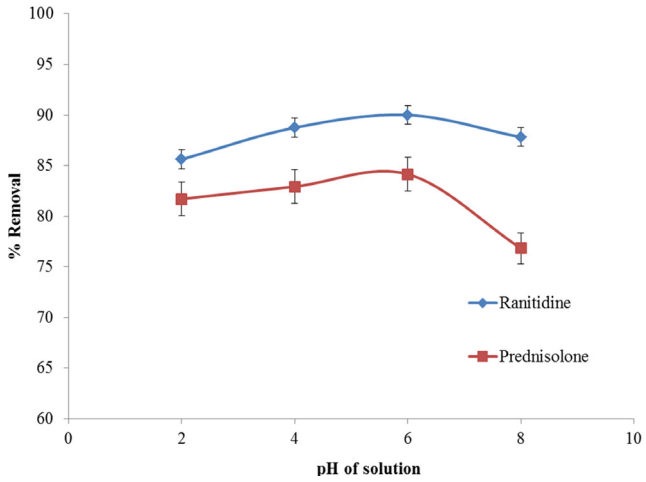

Fig. 4. Effect of pH on the removal of ranitidine and prednisolone present in solution.

facilitated by a parallel increase in the surface energy of the adsorbate moieties due to rise in temperature.

4.2.3. Effect of pH

The process of adsorption was greatly influenced by solution pH. Structural stability of the adsorbent depends on the charge and splitting of functional groups present on the surface of the adsorbent. Since solution pH may influence these properties, thus structural stability of the adsorbent is highly sensitive to alterations in solution pH [40]. In this study, percentage removal of both the adsorbate used (i.e, Ranitidine and Prednisolone) was determined over solution pH ranging from 2–8, as shown in Fig. 4. The % drug adsorption increased from 65.62–90.94% for ranitidine and 63.17–84.15% for prednisolone with a parallel increase in solution pH till pH 6 was reached. The process attained equilibrium after 60 min and a further increase of pH had no significant effect on % removal for both pharmaceuticals. This had mainly occurred due to electrostatic interactions between GO and adsorbate moieties [40,41]. The maximum % removal for ranitidine and prednisolone was found to be 90.94% and 84.15% when solution pH value was 6.

4.2.4. Effect of agitation speed

The effect of agitation speed was determined over a range of 80–140 rpm. Fig. 5 reveals that a rise in percentage drug removal ranging from 63.75–90.94% was recorded for Ranitidine with% percentage removal occurring at an agitation speed of 140 rpm. A similar rise in percentage removal of Prednisolone (45.12–69.27%) was observed while the maximum% drug removal was recorded with 120 rpm. A further increase of agitation speed beyond 140 rpm was found to have no significant effect on % removal of both adsorbate. Agitation may have prevented aggregation or overlapping of GO particles in turn providing higher surface area for adsorption and yielding higher percentages of drug removal.

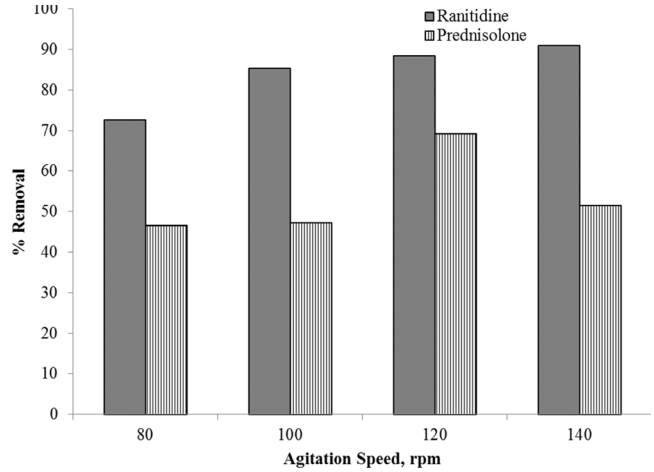

Fig. 5. Effect of agitation speed on the removal of ranitidine and prednisolone present in solution.

4.3. Adsorption isotherms

Schematic comparison between Langmuir and Freundlich data of both the drugs namely Ranitidine and Prednisolone has been presented in Table 1a. On the other hand, results of D-R and Temkin plots of both the drugs have been presented in Table 1b. Results indicated that Ranitidine adsorption by GO was guided by the Langmuir isotherms with highest regression coefficient value of 0.992. This reveals that the GO is of homogenous nature and the binding energy of each Ranitidine molecule on the surface GO was uniform. It also denoted that GO moieties were inert to each other and facilitated mono layer coverage formation of Ranitidine molecules on GO surfaces [42]. Moreover,the mean free energy, ε = 1.29 KJ/mol calculated from the D-R plot for Ranitidine adsorption indicated that the process was physiosorption in nature [39].

As evident from results shown in Table 1 (a and b), data obtained for Prednisolone adsorption by GO revealed a better fit to the Temkin isotherm model with a regression

Table 1 (a)
Langmuir and Freundlich model parameters for removal of Ranitidine & Prednisolone from aqueous solution using GO

	Langmuir				Freundlich		
	K_L (L/mg)	q_{max} (mg/g)	R_L	R^2	N	K_f (L/mg)	R^2
Ranitidine	0.00527	43.29	0.949	0.992	1.49	7.04	0.985
Prednisolone	0.00692	22.936	0.935	0.907	1.91	2.55	0.936

Table 1 (b)
Dubinin-Radushkevich and Temkin model parameters for removal of Ranitidine & Prednisolone from aqueous solution using GO

	Dubinin-Radushkevich				Temkin		
	q_m (mg/g)	β	ε (KJ/mol)	R^2	A_T (L/g)	B (J/mol)	R^2
Ranitidine	56.21	-3E-7	1.29	0.935	1.907	12.34	0.854
Prednisolone	13.18	2E-7	1.58	0.911	3.825	4.13	0.971

Table 2 (a)
Kinetic parameters for adsorption of Ranitidine Using GO

Pseudo first order			Pseudo second order			Intraparticle diffusion		
k_1 (min^{-1})	q_t (mg/g)	R^2	k_2 (min^{-1})	q_t (mg/g)	R^2	k_p	C (mg/g)	R^2
0.00095	1.88	0.997	0.043	8.85	0.998	0.1431	7.951	0.926

Table 2 (b)
Kinetic parameters for adsorption of Prednisolone Using GO

Pseudo first order			Pseudo second order			Intraparticle diffusion		
k_1 (min^{-1})	q_t (mg/g)	R^2	k_2 (min^{-1})	q_t (mg/g)	R^2	k_p	C (mg/g)	R^2
0.00146	0.634	0.991	0.197	4.78	0.999	0.0338	7.634	0.988

coefficient (R^2 = 0.971) higher than all other tested models. Best fit to Temkin isotherm indicated indirect adsorbent-adsorbate interactions on adsorption isotherms with a linear decrease of the heat of adsorption with coverage resulting from this interaction. Similar results have been reported previously [43].

4.4. Adsorption kinetics

One of the most essential parameter for describing the adsorption procedure is the adsorption kinetics. In this study, adsorption efficiency was found to increase with a corresponding increase in duration of treatment [38]. The adsorption of both ranitidine and prednisolone on the GO surface showed that the concerned process had reached equilibrium after a treatment period of 60 min. Data obtained were analyzed with pseudo first, second order and intra particle diffusion models. Results presented in Tables 2a and 2b revealed that adsorption of both drugs investigated in this study had demonstrated best fit to pseudo second order kinetic model with a regression co-efficient of 0.998 and 0.999 for Ranitidine and Prednisolone removal respectively.

4.5. Thermodynamic study

Changes in Gibb's free energy recorded for Ranitidine adsorption using GO has been clearly demonstrated in Table 3a. The negative ΔG° values obtained at all experimental temperatures confirmed the spontaneous nature of ranitidine adsorption by GO [39]. From the thermodynamic study it was found that calculated change in enthalpy (ΔH°) was negative (–62.604.2 kJ/mole) which in turn indicated that the adsorption was exothermic as well as physical in nature (involving weak forces of attraction). It therefore demonstrated that the process was energetically stable [30]. Furthermore, high value of ΔH° denoted the existence of a strong bonding between the adsorbate molecules and the adsorbent surface [29,42–45].

The changes recorded in Gibb's Free Energy for Prednisolone adsorption has been demonstrated in Table 3b. Values of ΔG° recorded at higher temperature clearly indicated the

spontaneous nature of Prednisolone adsorption by GO. Results obtained for Prednisolone adsorption showed similar thermodynamic behavior as that of observed in case of Ranitidine. A negative value for change in enthalpy (ΔH°) (–113.949 kJ/mole) indicated that the adsorption process was exothermic as well as physical in nature (involved weak forces of attraction).

4.6. Reusability of adsorbent

To investigate the reusability of the adsorbent, regeneration study is also very important. In this study, water, sodium hydroxide (10%), hydrochloric solution (10%), sodium chloride (10%) was used. It was observed that using sodium hydroxide, the recovery of pharmaceutical product from adsorbent was higher. After 5 adsorption and desorption study, it was observed that the removal efficiency of Ranitidine was 87.6% and Prednisolone was 71.3% [38].

Table 3 (a)
Thermodynamic parameters for adsorption of Ranitidine using GO

ΔG° (J mol^{-1})				ΔH° (KJ mol^{-1})	ΔS° (J $mole^{-1}$ K^{-1})
298K	303K	308K	313K	–62.6042	220.67
–3687.62	–3903.88	–4443.32	–7185.62		

Table 3 (b)
Thermodynamic parameters for adsorption of Prednisolone using GO

ΔG° (J mol^{-1})				ΔH° (KJ mol^{-1})	ΔS° (J $mole^{-1}$ K^{-1})
298K	303K	308K	313K	–113.949	380.35
198.31	–242.02	–4096.80	–4855.98		

4.7. ANN study

The Liebenberg-Marquardt back-propagation (LMBP) algorithm yielded the highest values of correlation coefficient (R^2 = 0.929 for Ranitidine and R^2 = 0.883 for Prednisolone) in comparison to other tested models like conjugate gradient back-propagation with Polak-Ribie´re, scaled conjugate gradient, resilient back-propagation. Results of the ANN analysis obtained using the LMBP algorithm has been shown in Figs. 6a and 6b. Both Fig. 6a and 6b show a comparative analysis of calculated and experimental values of output variables obtained from the test data by using the neural network model. The high correlation coefficient values determined for the calculated and experimental data indicated that data recorded for adsorption of both drugs were within experimental ranges and demonstrated best fit to the neural network model reported in this study [33,43].

5. Conclusion

The present study established the high potential and efficiency of GO nanoplatelets as an adsorbent for efficient adsorption of two adsorbates namely Ranitidine and Prednisolone. The result obtained for adsorption of both the pharmaceuticals showed the adsorption efficiency of GO to be quite high. Batch adsorption experiments are carried out to study different process parameters and their influences on the process efficiency. The highest removal efficiency was found to be 90.04% and 92.68% in case of Ranitidine

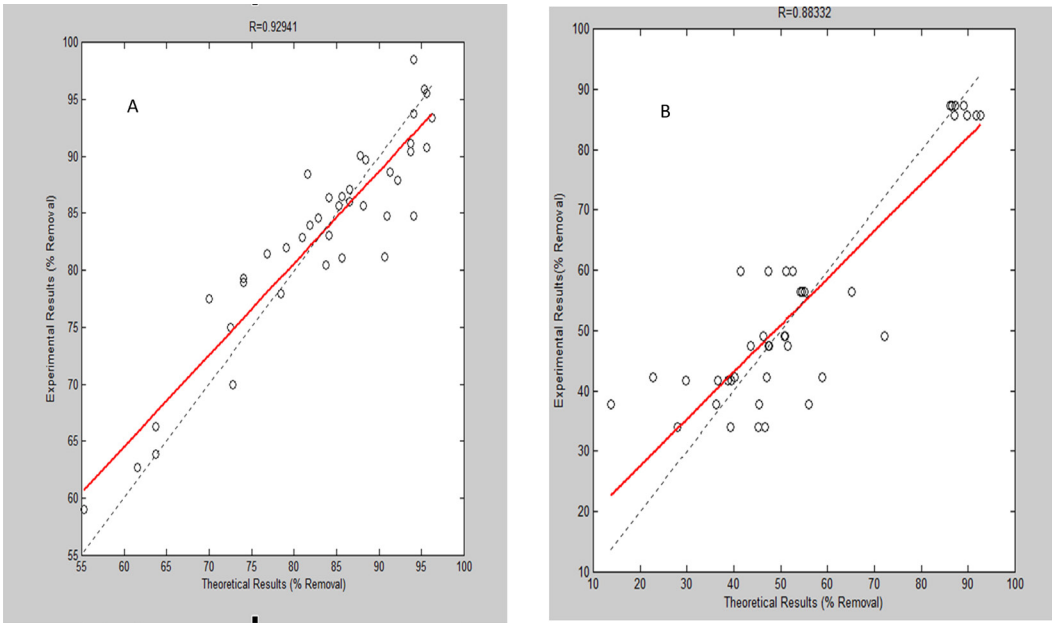

Fig. 6. a. ANN figure on removal of ranitidine using GO; b. ANN figure on removal of prednisolone using GO.

and Prednisolone respectively. The maximum removal of ranitidine was observed under an initial Ranitidine concentration of 10 mg/L, adsorbent (GO) dosage of 1.00 g/L, solution pH 6, agitation speed of 140 rpm and temperature of 313K after a treatment period of 60 min. All other parameters favoring maximum removal of Prednisolone was same as that for adsorption of Ranitidine, excepting the agitation speed and adsorbent dosage. Optimum values of agitation speed and adsorbent dosage facilitating maximum Prednisolone adsorption was 120 rpm and 2.00 g/L of GO respectively. The process of pharmaceutical uptake by GO was guided by Langmuir isotherm model for ranitidine adsorption and Temkin isotherm for Prednisolone adsorption. Results obtained in this study also revealed that the adsorption of both drugs demonstrated best fit to pseudo second order kinetics. Analysis of thermodynamic parameters established that the process of adsorption for both the drugs was spontaneous, physisorption and endothermic in nature. Hence it may be concluded that grapheme-oxide (GO) is a potential adsorbent for the effective removal of pharmaceuticals like Ranitidine and Prednisolone owing to the efficient adsorption capacity demonstrated by it in very small dosage as well as remarkably less treatment time.

Acknowledgement

Papita Das and Subrata Kumar Majumder are thankful to Department of Science and Technology –WTI, Government of India (DST/TM/WTI/2K16/20) for the financial support. The authors are thankful to all the members of Department of Chemical Engineering, Jadavpur University.

Symbols

C_i & C_e	—	Initial & equilibrium concentrations (mg L^{-1}) of adsorbate in the solution
V	—	Amount of solution taken and m (g) is the mass of adsorbent used
m (g)	—	Mass of adsorbent used
q_e (mg·g^{-1})	—	Solid phase concentrations of adsorbate at equilibrium
C_e (mg·L^{-1})	—	Liquid-phase concentrations of adsorbate at equilibrium
q_{max}(mg·g^{-1})	—	Maximum adsorption capacity
K_L (L·mg^{-1})	—	Langmuir constant
K_F (mg·g^{-1}) (L·mg^{-1}) & $1/n$	—	Freundlich constants related to adsorption capacity
n	—	Heterogeneity factor calculated by plotting $\ln(q_e)$ linearly against $\ln C_e$
β (mol²·K^{-1}·J^{-2})	—	Activity coefficient
ε	—	The Polanyi potential
E (KJ mol^{-1})	—	The mean sorption energy
A_T (L·g^{-1})	—	Temkin isotherm equilibrium binding constant
B (J·mol^{-1})	—	Constant related to heat of sorption
t	—	Time
q_1 & q_t (mol g^{-1})	—	Amounts of adsorbate adsorbed on adsorbent at equilibrium and at various times
k_1 (min^{-1})	—	Rate constant of the first-order model for the adsorption process
q_2 (mol g^{-1})	—	Maximum adsorption capacity for the pseudo-second-order adsorption
k_2 (g mol^{-1} min^{-1})	—	Rate constant of the pseudo-second-order model for the adsorption process C = intercept
k_p (mol g^{-1} $min^{-1/2}$)	—	Intra particle diffusion rate constant
K_C	—	Equilibrium constant
C_A (mol dm^{-3})	—	Amount of dye adsorbed on the adsorbent of the solution at equilibrium
C_S (mol dm^{-3})	—	Equilibrium concentration of the dye in the solution
T (K)	—	Solution temperature
R	—	Gas constant
ΔH^o	—	Enthalpy
ΔS^o	—	Entropy

Abbreviations

ANN	—	Artificial neural network
D-R	—	Dubinin-Radushkevich
FTIR	—	Fourier Transform Infrared spectroscopy
GO	—	Graphene Oxide
LMBP	—	Liebenberg-Marquardt back-propagation
SEM	—	Scanning Electron Microscope
XRD	—	X-ray Diffraction

References

[1] J.R. Utrilla, M.S. Polo, M.Á.F. García, G. PJoya, R.O. Pérez, Pharmaceuticals as emerging contaminants and their removal from water. A review, Chemosphere, 93(7) (2013) 1268–1287.
[2] A. Sangion, P. Gramatica, PBT assessment and prioritization of contaminants of emerging concern: Pharmaceuticals, Env. Res., 147 (2016) 297–306.
[3] J. Wang, L. Chu, Irradiation treatment of pharmaceutical and personal care products (PPCPs) in water and wastewater: an overview, Rad. Phys. Chem., 125 (2016) 56–64.
[4] T. Lin, S. Yu, W. Chen, Occurrence, removal and risk assessment of pharmaceutical and personal care products (PPCPs) in an advanced drinking water treatment plant (ADWTP) around Taihu Lake in China, Chemosphere, 152 (2016) 1–9.
[5] P. Das, P. Das, Graphene oxide for the treatment of ranitidine containing solution: optimum sorption kinetics by linear and nonlinear methods and simulation using artificial neural network, Proc. Saf. Environ. Prot., 102 (2016) 589–595.
[6] M. Dutta, U. Das, S. Mondal, S. Bhattachriya, R. Khatun, R. Bagal, Adsorption of acetaminophen by using tea waste derived activated carbon, Inter. J. Environ. Sci., 6(2) (2015) 270.
[7] D.W. Kolpin, E.T. Furlong, M.T. Meyer, E.M. Thurman, S.D. Zaugg, L.B. Barber, H.T. Buxton, Pharmaceuticals, hormones, and other organic wastewater contaminants in US streams, 1999–2000: A national reconnaissance, Environ. Sci. Technol., 36(6) (2002) 1202–1211.
[8] K. Mphahlele, M.S. Onyango, S.D. Mhlanga, S.D. Adsorption of aspirin and paracetamol from aqueous solution using Fe/N-CNT/β-cyclodextrin nanocomopsites synthesized via a benign microwave assisted method, J. Environ. Chem. Eng., 3(4) (2015) 2619–2630.

[9] S.E. Kuh, D.S. Kim, Removal characteristics of cadmium ion by waste egg shell, Environ. Technol., 21(8) (2000) 883–890.
[10] J.J.M. Órfão, A.I.M. Silva, J.C.V. Pereira, S.A. Barata, I.M. Fonseca, P.C.C. Faria, M.F.R. Pereira, Adsorption of a reactive dye on chemically modified activated carbons—influence of pH, J. Coll. Interf. Sci., 296(2) (2006) 480–489.
[11] M. Valix, W.H. Cheung, G. McKay, Preparation of activated carbon using low temperature carbonisation and physical activation of high ash raw bagasse for acid dye adsorption, Chemosphere, 56(5) (2004) 493–501.
[12] N. Pramanpol, N. Nitayapat, Adsorption of reactive dye by eggshell and its membrane, Kasetsart J., 40 (2006) 192–197.
[13] F.A. Batzias, D.K. Sidiras, Dye adsorption by calcium chloride treated beech sawdust in batch and fixed-bed systems, J. Hazard. Mater., 114(1–3) (2004) 167–174.
[14] K. Chojnacka, Biosorption of Cr (III) ions by eggshells, J. Hazard. Mater., 121(1–3) (2005) 167–173.
[15] S. Papić, N. Koprivanac, A.L. Božić, A. Meteš, Removal of some reactive dyes from synthetic wastewater by combined Al (III) coagulation/carbon adsorption process, Dyes Pigm., 62(3) (2004) 291–298.
[16] W.T. Tsai, J.M. Yang, C.W. Lai, Y.H. Cheng, C.C. Lin, C.W. Yeh, Characterization and adsorption properties of eggshells and eggshell membrane, Biores Technol., 97(3) (2006) 488–493.
[17] K. Vijayaraghavan, J. Jegan, K. Palanivelu, M. Velan, M. Removal and recovery of copper from aqueous solution by eggshell in a packed column, Miner. Eng., 18(5) (2005) 545–547.
[18] M. MEl Zawahry, M.M. Kamel, M.M. Removal of azo and anthraquin one dyes from aqueous solutions by Eichhorniacrassipes, Wat Res., 38(13) (2004) 2967–2972.
[19] A. Vona, F. di Martino, J. GIvars, Y. Picó, J.A. Mendoza-Roca, M. I. Iborra-Clar, Comparison of different removal techniques for selected pharmaceuticals, J. Wat. Process Eng., 5 (2015) 48–57.
[20] A. Mirzaei, Z. Chen, F. Haghighat, L. Yerushalmi, Removal of pharmaceuticals from water by homo/heterogonous Fenton-type processes–A review, Chemosphere, 174 (2017) 665–688.
[21] G. Zhao, L. Jiang, Y. He, J. Li, H. Dong, X. Wang, W. Hu, Sulfonated graphene for persistent aromatic pollutant management, Adv. Mater., 23(34) (2011) 3959–3963.
[22] Z. Jin, X. Wang, Y. Sun, Y. Ai, X. Wang, Adsorption of 4-n-nonylphenol and bisphenol-A on magnetic reduced graphene oxides: a combined experimental and theoretical studies, Environ. Sci. Technol., 49(15) (2015) 9168–9175.
[23] S. Yu, X. Wang, Y. Ai, X. Tan, T. Hayat, W. Hu, X. Wang, X. Experimental and theoretical studies on competitive adsorption of aromatic compounds on reduced graphene oxides, J. Mater. Chem. A., 4(15) (2016) 5654–5662.
[24] Y. Yoon, W.K. Park, T.M. Hwang, D.H. Yoon, W.S. Yang, J.W. Kang, Comparative evaluation of magnetite–graphene oxide and magnetite-reduced graphene oxide composite for As (III) and As (V) removal, J. Hazard. Mater., 304 (2016) 196–204.
[25] S. Yu, X. Wang, W. Yao, J. Wang, Y. Ji, Y. Ai, Y. A. Alsaedi, T. Hayat, X. Wang, X, Macroscopic, spectroscopic, and theoretical investigation for the interaction of phenol and naphthol on reduced graphene oxide, Environ Sci. Technol., 51(6) (2017) 3278–3286.
[26] X. Cai, S. Tan, A. Xie, M. Lin, Y. Liu, X. Zhang, Z. Lin, T. Wu, W. Mai, W. Conductive methyl blue-functionalized reduced graphene oxide with excellent stability and solubility in water, Mater Res Bull., 46(12) (2011) 2353–2358.
[27] X. Zhao, X. Zou, L. Ye, Controlled pH-and glucose-responsive drug release behavior of cationic chitosan based nano-composite hydrogels by using graphene oxide as drug nanocarrier, J. Ind. Eng. Chem., 49 (2017) 36–45.
[28] P.D. Saha, S. Dutta, S. Mathematical modeling of biosorption of safranin onto rice husk in a packed bed column using artificial neural network analysis, Desal. Wat. Treat., 41 (2012) 308–314.
[29] G.K. Ramesha, A.V. Kumara, H.B. Muralidhara, S. Sampath, S. Graphene and graphene oxide as effective adsorbents toward anionic and cationic dyes, J. Colloid. Interf. Sci., 361(1) (2011) 270–277.
[30] K. Sinha, S. Chowdhury, P.D. Saha, S. Datta, Modeling of microwave-assisted extraction of natural dye from seeds of Bixaorellana (Annatto) using response surface methodology (RSM) and artificial neural network (ANN), Ind. Crop Prod., 41 (2013) 165–171.
[31] M. Mukherjee, S. Goswami, P. Banerjee, S. Sengupta, P. Das, P.K. Banerjee, P.K.S. Datta, Ultrasonic assisted graphene oxide nanosheet for the removal of phenol containing solution, Environ. Technol. Innov., (2017) DOI: 10.1016/j.eti.2016.11.006.
[32] S. Goswami, P. Banerjee, S. Datta, A. Mukhopadhayay, A.P. Das, Graphene oxide nanoplatelets synthesized with carbonized agro-waste biomass as green precursor and its application for the treatment of dye rich wastewater, Proc. Saf. Environ Prot, 106 (2017) 163–172.
[33] P. Banerjee, S.R. Barman, A. Mukhopadhayay, P. Das, Ultrasound assisted mixed azo dye sorption by chitosan–graphene oxide nanocomposite, Chem. Eng. Res. Design., 117 (2017) 43–56.
[34] S. Roy, S. Manna, S. Sengupta, A. Ganguli, S. Gowami, P. Das, Comparative assessment on Defluoridation of wastewater using chemical and bio-reduced graphene oxide: Batch,thermodynamic, kinetics and optimization using response surface methodology and artificial neural network, Proc. Saf. Environ. Prot., 111 (2017) 221–231.
[35] S. Lagergren, About the theory of so-called adsorption of soluble substances. KungligaSvenskaVetenskapsakademiensHandlingar, 24 (1898) 1–39.
[36] Y.S. Ho, G. McKay, Pseudo-second-order model for sorption-processes, Proc. Biochem., 34 (1999) 451–465.
[37] G. McKay, The adsorption of dye stuffs from aqueous solution using activated carbon: analytical solution for batch adsorption based on external mass transfer and pore diffusion,. Chem. Eng. J., 27 (1983) 187–196.
[38] P. Banerjee, P. Das, A. Zaman, P. Das, Application of graphene oxide nanoplatelets for adsorption of ibuprofen from aqueous solutions: Evaluation of process kinetics and thermodynamics, Process Saf. Environ. Prot., 101 (2016) 45–53.
[39] R. Rathour, P. Das, K. Aikat, Microwave-assisted synthesis of graphene and its application for adsorptive removal of malachite green: thermodynamics, kinetics and isotherm study, Desal. Water Treat., 57(9) (2016) 7312–7321.
[40] A. Özcan, E.M. Öncü, A.S. Özcan, Kinetics, isotherm and thermodynamic studies of adsorption of Acid Blue 193 from aqueous solutions onto natural sepiolite, Colloids Surf A: Physicochem Eng. Asp., 277(1–3) (2006) 90–97.
[41] A. Tadjarodi, S.M. Ferdowsi, R.Z. Dorabei, A. Barzin, Highly efficient ultrasonic-assisted removal of Hg (II) ions on graphene oxide modified with 2-pyridinecarboxaldehyde thiosemicarbazone: adsorption isotherms and kinetics studies, Ultrason Sonochem., 33 (2016) 118–128.
[42] M. Ghaedi, A. Ansari, F. Bahari, A.M. Ghaedi, A. Vafaei, A hybrid artificial neural network and particle swarm optimization for prediction of removal of hazardous dye brilliant green from aqueous solution using zinc sulfide nanoparticle loaded on activated carbon, Spectrochim Acta A Mol Biomol Spectrosc., 137 (2015) 1004–1015.
[43] P. Banerjee, S. Sau, P. Das, A. Mukhopadhayay, A. Optimization and modelling of synthetic azo dye wastewater treatment using Graphene oxide nanoplatelets: characterization toxicity evaluation and optimization using artificial neural network, Ecotoxicol. Environ. Saf., 119 (2015) 47–57.
[44] G.K. Ramesha, A.V. Kumara, H.B. Muralidhara, S. Sampath, Graphene and graphene oxide as effective adsorbents toward anionic and cationic dyes, J. Colloid Interface Sci., 361(1) (2011) 270–277.
[45] H.N. Bhatti, A. Jabeen, M. Iqbal, S. Noreen, Z. Naseem, Adsorptive behavior of rice bran-based composites for malachite green dye: Isotherm, kinetic and thermodynamic studies, J. Mol. Liq., 237 (2017) 322–333.